

# Localized Orbital Scaling Correction with Linear Response in Materials

Jacob Z. Williams<sup>†</sup> and Weitao Yang<sup>\*,†,‡</sup>

<sup>†</sup>*Department of Chemistry, Duke University, Durham, NC 27708, USA*

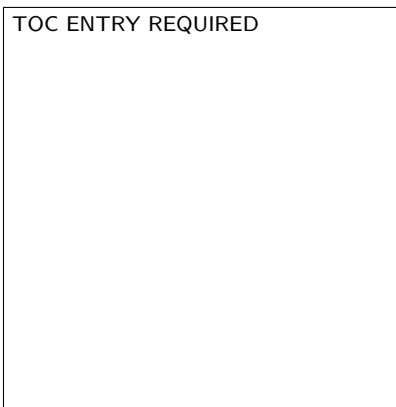
<sup>‡</sup>*Department of Physics, Duke University, Durham, NC 27708, USA*

E-mail: [weitao.yang@duke.edu](mailto:weitao.yang@duke.edu)

## Abstract

Density functional theory (DFT) is a powerful tool for quantum-mechanical calculations, but practical calculations suffer systematic errors like incorrect charge densities and total energies in molecular dissociation, underestimated band gaps in bulk materials, and poor energy level alignment at interfaces. These problems are due to delocalization error. The localized orbital scaling correction (LOSC) removes delocalization error in molecules effectively, but screening of the Hartree-exchange-correlation response is necessary to correct it in materials. We introduce LOSC with system-dependent linear-response screening (lrLOSC), which effectively corrects delocalization error in semiconductors and insulators. After correcting for electron-phonon effects, the band gaps of eleven test systems are predicted with a mean absolute error of 0.28 eV, comparable to self-consistent *GW*. This method represents a significant step forward in correcting densities and total energies across system sizes and solving the band gap and energy level alignment problems entirely within the DFT framework.

## TOC Graphic



Density functional theory (DFT)<sup>1–5</sup> is rightly regarded as the default method for quantum-mechanical calculations in both chemistry and materials science. It features a combination of reasonably accurate density functional approximations (DFAs) and efficient computational implementations that remains unparalleled decades later. But DFAs suffer systematic errors, including a characteristic and enduring underestimation of the fundamental (band) gap.<sup>6</sup> Accurately computing this gap—and the orbital energies (energy bands) from which it is obtained<sup>7–9</sup>—is critical for calculations involving semiconductors;<sup>10,11</sup> solar cells;<sup>12</sup> photocatalysts;<sup>13</sup> and interfaces,<sup>14,15</sup> across which energy bands are renormalized. Behind the band gap problem lies delocalization error.<sup>16–19</sup>

Delocalization error in DFAs is a significantly and systematically incorrect behavior of the energy  $E$  viewed as a function of the number  $N$  of electrons, but it looks different depending on the size of the system.<sup>16</sup> The exact  $E(N)$  curve is piecewise linear, with derivative discontinuities at integer  $N$ ; the magnitude of the discontinuity gives the band gap.<sup>7,20</sup> When calculated with typical DFAs,  $E(N)$  is convex for small finite systems, underestimating the derivative discontinuity and thus the gap. In periodic boundary conditions, piecewise linearity of  $E(N)$  is restored automatically, but deceptively: the electron delocalizes into the infinite lattice, the derivative discontinuity is underestimated just like for finite  $N$ , and the total energy of charged bulk systems is incorrect.<sup>16</sup> Correcting delocalization error in both molecules and materials, then, requires that both the orbital energies and the total energy be corrected, all within the same framework of approximations.

Two ingredients, orbital localization and screening, are key to delocalization error corrections. The localized orbital scaling correction (LOSC) initially featured localization without screening,<sup>21,22</sup> which is good enough to cure delocalization error in the valence orbitals of atoms and small molecules.<sup>23</sup> LOSC orbital energies have accuracy comparable to  $GW$  methods in molecules,<sup>24</sup> and the LOSC orbital energies can replace  $GW$  quasiparticle energies as the starting point for Bethe–Salpeter calculations of neutral excitations.<sup>25</sup> Screening without localization is realized by the global scaling correction (GSC).<sup>26,27</sup> GSC with screen-

ing, which treats delocalization error in atoms and molecules, is based on the exact second derivatives of the total energy with respect to the orbital occupation number.<sup>28</sup> It improves calculated photoemission spectra,<sup>29</sup> similar to prior work on valence orbital energies, when orbital relaxation is included.<sup>27,30,31</sup> Although screening plays a smaller role in the valence orbital ionization of molecules,<sup>29</sup> both localization and screening are necessary to describe core-electron quasiparticle energies accurately.<sup>32</sup>

Both localization and screening are also necessary to correct delocalization error in bulk materials. GSC, lacking localization, offers no correction at all to the total energy of bulk semiconductors and insulators. On the other hand, the initial version of LOSC significantly overestimates the correction to the orbital energies because screening of the Coulomb repulsion by other electrons is ignored. Mahler et al.<sup>33</sup> proposed screened LOSC (sLOSC), which included an empirically screened Hartree repulsion and substantially improved the band gaps of semiconductors and insulators. But sLOSC’s screening is identical for all systems, fundamentally limiting its accuracy. In this work, paralleling similar development for finite systems,<sup>32</sup> we extend LOSC to include the linear-response screening of GSC: we call the resulting method lrLOSC. We note the similarity of lrLOSC to Koopmans-compliant spectral functionals,<sup>34–36</sup> the Wannier–Koopmans method,<sup>37–41</sup> and Wannier optimally-tuned screened range-separated hybrid functionals,<sup>42,43</sup> all of which correct orbital energies using localized orbitals (in materials, Wannier functions) and screening of the electron-electron interaction. Unlike LOSC, however, these functionals do not correct the total energy of systems with integer orbital occupations, such as physical systems with a finite band gap.<sup>34</sup> Thus, their correction cannot be size-consistent for molecular dissociation.<sup>21</sup>

lrLOSC modifies the DFA total energy by

$$\Delta E = \frac{1}{2} \sum_{\sigma} \sum_{ij\mathbf{R}} \lambda_{\mathbf{R}ij\sigma}^* (\delta_{\mathbf{R}ij} - \lambda_{\mathbf{R}ij\sigma}) \kappa_{\mathbf{R}ij\sigma}, \quad (1)$$

where  $i, j, \sigma$  are respectively the band-like and spin indices of localized orbitals  $|w_{\mathbf{R}i\sigma}\rangle$  and

$\mathbf{R}$  indexes the primitive cell translation vectors (see below). The local occupations  $\lambda_{\mathbf{R}ij\sigma} = \langle w_{\mathbf{0}i\sigma} | \rho | w_{\mathbf{R}j\sigma} \rangle$  are elements of the density matrix  $\rho$  in the local orbital basis, and the curvature  $\kappa_{\mathbf{R}ij\sigma}$  measures the delocalization error between  $|w_{\mathbf{0}i\sigma}\rangle$  and  $|w_{\mathbf{R}j\sigma}\rangle$ .  $\delta_{\mathbf{R}ij}$  is the Kronecker delta, and  $\lambda^*$  is the complex conjugate of  $\lambda$ . Note that lrLOSC assumes a spin-polarized, collinear DFA calculation, with orthogonal Bloch spin orbitals:  $\langle \psi_{\mathbf{k}m\sigma} | \psi_{\mathbf{q}n\tau} \rangle \propto \delta_{\mathbf{k}\mathbf{q}} \delta_{mn} \delta_{\sigma\tau}$ .

LOSC's localized orbitals are called orbitalets in finite systems<sup>22</sup> and dually localized Wannier functions (DLWFs) in periodic boundary conditions.<sup>44</sup> DLWFs are generalized Wannier functions<sup>45</sup> constructed from the Kohn–Sham Bloch orbitals  $|\psi_{\mathbf{k}n\sigma}\rangle$ , where  $\mathbf{k}$  indexes the  $N_k$  points sampled from the irreducible Brillouin zone,  $n$  the electronic bands, and  $\sigma$  the spin, as

$$|w_{\mathbf{R}i\sigma}\rangle = \frac{1}{N_k} \sum_{\mathbf{k}} e^{-i\mathbf{k}\cdot\mathbf{R}} \sum_n U_{ni}^{\mathbf{k}} |\psi_{\mathbf{k}n\sigma}\rangle. \quad (2)$$

The DLWFs are periodic on a supercell  $N_k$  times larger than the primitive unit cell and are indexed by a band-like index  $i$  and a primitive cell translation vector  $\mathbf{R}$ . At each  $\mathbf{k}$ -point, the unitary operator  $U^{\mathbf{k}}$  is chosen to minimize the cost function

$$F = \sum_i [(1 - \gamma)\Delta r_{\mathbf{0}i\sigma}^2 + \gamma\Delta h_{\mathbf{0}i\sigma}^2], \quad (3)$$

where  $\Delta r_{\mathbf{0}i\sigma}^2$  is the spatial variance  $\langle w_{\mathbf{0}i\sigma} | \mathbf{r} | w_{\mathbf{0}i\sigma} \rangle^2 - \langle w_{\mathbf{0}i\sigma} | r^2 | w_{\mathbf{0}i\sigma} \rangle$  and  $\Delta h_{\mathbf{0}i\sigma}^2$  is the energy variance. The numerical value of  $\gamma$  depends on the units chosen, but all LOSC results to date have used the same value; when  $\Delta r^2$  is computed in  $a_0^2$  and  $\Delta h^2$  in  $\text{eV}^2$ ,  $\gamma = 0.47714$ . (Setting  $\gamma = 0$  recovers maximally localized Wannier functions.<sup>46</sup>) Despite being spatially localized, DLWFs retain information about the energy spectrum, necessary for describing chemical reactivity.<sup>47</sup> DLWFs can be constructed for both metals and semiconductors because they do not require separation of the valence and conduction manifolds.<sup>21,22,44</sup>

In finite systems, the curvature is  $\kappa_{nn\sigma} = \partial^2 E / \partial f_{n\sigma}^2$ , where  $f_{n\sigma}$  is the occupation of the Kohn–Sham orbital  $|\psi_{n\sigma}\rangle$ . When  $|\psi_{n\sigma}\rangle$  is a frontier orbital,  $\partial^2 E / \partial f_{n\sigma}^2$  describes the deviation of  $E(N)$ , computed by a DFA, from the correct linear behavior, including the

effect of screening by all other electrons (also called orbital relaxation).<sup>28</sup> The original GSC method approximated  $\kappa_{nn\sigma}$ , treating only the Coulomb interaction, and used Kohn–Sham orbital densities instead of the Fukui function  $\partial\rho_\sigma/\partial f_{n\sigma}$ .<sup>26,27</sup> Yang et al.<sup>28</sup> extended the result to include the exchange–correlation interaction, finding the exact second-order derivatives to be

$$\kappa_{nn\sigma} = \langle \rho_{n\sigma} | \sum_{\tau} (\epsilon^{\tau})^{-1} f_{\text{Hxc}}^{\tau\sigma} | \rho_{n\sigma} \rangle = \langle \rho_{n\sigma} | f_{\text{Hxc}}^{\sigma\sigma} + \sum_{\nu\tau} f_{\text{Hxc}}^{\sigma\nu} \chi^{\nu\tau} f_{\text{Hxc}}^{\tau\sigma} | \rho_{n\sigma} \rangle. \quad (4)$$

Here,  $\rho_{n\sigma}(\mathbf{r}) = |\psi_{n\sigma}(\mathbf{r})|^2$  is the density of the Kohn–Sham orbital  $|\psi_{n\sigma}\rangle$ ;  $(\epsilon^{\tau})^{-1}(\mathbf{r}, \mathbf{r}')$  is the inverse static microscopic dielectric function;

$$f_{\text{Hxc}}^{\sigma\nu}(\mathbf{r}, \mathbf{r}') = \frac{\delta^2 E_{\text{Hxc}}}{\delta\rho^{\sigma}(\mathbf{r})\delta\rho^{\nu}(\mathbf{r}')} = \frac{1}{|\mathbf{r} - \mathbf{r}'|} + \frac{\delta^2 E_{\text{xc}}}{\delta\rho^{\sigma}(\mathbf{r})\delta\rho^{\nu}(\mathbf{r}')} \quad (5)$$

is the Hartree–exchange–correlation kernel; and

$$\chi^{\nu\tau}(\mathbf{r}, \mathbf{r}') = \frac{\delta\rho^{\nu}(\mathbf{r})}{\delta v^{\tau}(\mathbf{r}')} = \frac{\delta^2 E}{\delta v^{\nu}(\mathbf{r})\delta v^{\tau}(\mathbf{r}')} \quad (6)$$

is the response of the density to an external perturbing potential  $\delta v$ , to linear order. Observe that the curvature is given by a bare kernel  $f_{\text{Hxc}}$  screened by the inverse dielectric function  $\epsilon^{-1}$ , or equivalently by the sum of the bare kernel and a relaxed kernel modulated by  $\chi$ . This curvature was implemented in the most recent iteration of GSC, known as GSC2.<sup>29</sup> Compared to the initial implementation, including orbital relaxation modestly improves the performance of GSC, reducing the error in ionization energy and electron affinity for small molecules by an average of about 0.2 eV. GSC2 still gives no correction to the total energy for materials; its screened interaction must be combined with the localized DLWFs. In molecules, including both the screening of Equation (4) and localization greatly improves the energies of core-orbital quasiparticles.<sup>32</sup>

In LOSC, the GSC2 curvature is transformed to the DLWF basis; its matrix elements

are

$$\kappa_{\mathbf{R}ij\sigma} = \langle \rho_{\mathbf{0}i\sigma} | f_{\text{Hxc}}^{\sigma\sigma} + \sum_{\nu\tau} f_{\text{Hxc}}^{\sigma\nu} \chi^{\nu\tau} f_{\text{Hxc}}^{\tau\sigma} | \rho_{\mathbf{R}j\sigma} \rangle, \quad (7)$$

where  $\rho_{\mathbf{R}j\sigma}(\mathbf{r}) = |w_{\mathbf{R}j\sigma}(\mathbf{r})|^2$  is a DLWF density. Note that  $\kappa$  in LOSC is not diagonal because the DLWFs are not Kohn–Sham eigenfunctions. These off-diagonal elements allow interactions between pairs of orbitals to affect the total energy, even at long range. The analogous elements for canonical orbitals were derived as cross-terms  $\partial^2 E / \partial f_{n\sigma} \partial f_{m\sigma}$  in the GSC2 method (see the Supporting Information of Mei et al.<sup>29</sup>). In lrLOSC, we compute  $\kappa_{\mathbf{R}ij\sigma}$  using density functional perturbation theory;<sup>48</sup> this reduces the computational cost by a factor of  $N_k$ , the number of  $\mathbf{k}$ -points, because both curvature elements linear in DLWF densities<sup>49</sup> and the densities themselves<sup>36</sup> decompose monochromatically. Thus

$$\kappa_{\mathbf{R}ij\sigma} = \frac{1}{N_k} \sum_{\mathbf{q}} e^{-i\mathbf{q}\cdot\mathbf{R}} \left[ \langle \rho_{\mathbf{0}i\sigma}^{\mathbf{q}} | V_{\mathbf{0}j\sigma}^{\mathbf{q}} \rangle + \sum_{\tau} \langle \delta\rho_{\mathbf{0}i\tau}^{\mathbf{q}} | V_{\mathbf{0}j\tau}^{\mathbf{q}} \rangle \right], \quad (8)$$

where  $\mathbf{q}$  samples the Brillouin zone uniformly including its origin, and

$$V_{\mathbf{0}j\tau}^{\mathbf{q}}(\mathbf{r}) = \int d\mathbf{r}' f_{\text{Hxc}}^{\tau\sigma}(\mathbf{r}, \mathbf{r}') \rho_{\mathbf{0}j\sigma}^{\mathbf{q}}(\mathbf{r}'), \quad (9)$$

$$\delta\rho_{\mathbf{0}i\tau}^{\mathbf{q}}(\mathbf{r}') = \sum_{\nu} \int d\mathbf{r} \chi^{\tau\nu}(\mathbf{r}, \mathbf{r}') V_{\mathbf{0}i\nu}^{\mathbf{q}}(\mathbf{r}'). \quad (10)$$

See the Supporting Information for the details of this derivation.

We compute lrLOSC total and band energy corrections on a set of eleven semiconductors and insulators. DFA calculations are performed with Quantum ESPRESSO,<sup>50–52</sup> version 7.1. We use the PBE functional,<sup>53</sup> optimized norm-conserving Vanderbilt pseudopotentials<sup>54</sup> built under PBE with scalar relativistic corrections, a wavefunction kinetic energy cutoff of 75 Ry, and a  $6 \times 6 \times 6$  Monkhorst–Pack sampling of the irreducible Brillouin zone.

Computing  $|\delta\rho_{\mathbf{0}i\tau}^{\mathbf{q}}\rangle$  occupies the vast majority of lrLOSC’s computational time. For each  $|\rho_{\mathbf{0}i\tau}^{\mathbf{q}}\rangle$ , there are  $N_{\text{occ}}$  coupled equations that must be solved at each  $\mathbf{k}$ -point, for a total runtime scaling as  $\mathcal{O}(N_{\text{DLWF}} N_{\mathbf{k}}^2 N_{\text{occ}}^3)$  (since  $N_{\mathbf{q}} = N_{\mathbf{k}}$ ).

The Hartree kernel is computed in reciprocal space, where the Coulomb repulsion is diagonal; its divergence is corrected after integration by the method of Gygi and Baldereschi<sup>55</sup>. The divergence correction to  $\langle \delta\rho_{\mathbf{0}i\sigma}^{\mathbf{q}} | V_{\mathbf{0}j\sigma}^{\mathbf{q}} \rangle$  must be scaled by the macroscopic dielectric constant  $\epsilon_{\infty}$ , which is computed in `Quantum ESPRESSO`'s `PHonon` module, with the same computational parameters. The energy cutoff and Brillouin zone sampling were chosen to converge  $\epsilon_{\infty}$  to 0.01, and the valence band maximum and conduction band minimum to 0.01 eV.

DLWFs are obtained with a locally maintained fork<sup>44</sup> of `wannier90`,<sup>56–58</sup> and `lrLOSC` is implemented in a local fork of `Quantum ESPRESSO`'s development version. It adapts the `KCW` module,<sup>36</sup> leveraging its implementation of the monochromatic decomposition and its linear-response routines.

`lrLOSC` greatly improves fundamental gaps relative to PBE. Because `LOSC` is a purely electronic (Born–Oppenheimer) theory, its fundamental gap is not directly comparable to the experimental band gap. Even at zero temperature, coupling of the electrons to the lattice changes the gap, an effect called zero-point renormalization (ZPR).<sup>59–61</sup> ZPR usually narrows the gap slightly, but in some cases its effect can exceed 1 eV. We thus compare `lrLOSC` against the *electronic* gap, obtained by subtracting ZPR from the experimental gap, and it performs extremely well: the mean absolute error (MAE) on our test set is only 0.28 eV. This compares well with quasiparticle self-consistent *GW*, which yielded a MAE of about 0.46 eV on a similar set of materials.<sup>62</sup>

Note that  $\gamma$ , which describes the balance between spatial and energy localization of the DLWFs in Equation (3), is the only free parameter in `lrLOSC`. The value we use,  $\gamma = 0.47714$ , was originally optimized for `LOSC` in finite systems;<sup>22</sup> it is also used for `sLOSC` in materials.<sup>33</sup> It is interesting that our calculations show that it is also appropriate for `lrLOSC`.

Figure 2 shows the band structure of lithium fluoride calculated with PBE (left) and `lrLOSC` (right). The DFA gap is only 9.19 eV, much smaller than the electronic gap (15.43 eV, including a ZPR of  $-1.231$  eV). `lrLOSC` shifts occupied bands down and virtual bands up relative to the DFA and predicts a gap of 15.24 eV, within 0.2 eV of the electronic gap. `lr`

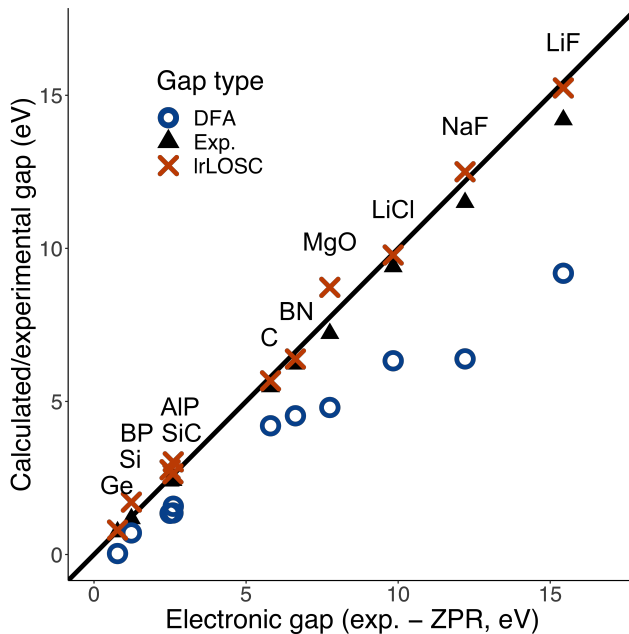


Figure 1: DFA, lrLOSC, and experimental gaps vs. electronic gap.

LOSC also improves the core-level energies, especially the lithium 1s state, compared to the parent DFA. Its performance is very similar in this system to the Koopmans-compliant Wannier functional;<sup>36</sup> it slightly outperforms  $G_0W_0$  in the electronic gap, but is outperformed in turn for the core-level energies.

**Table 1: Core-level quasiparticle energies and electronic gap of LiF by theory and experiment. The  $G_0W_0$  results are from LDA rather than PBE.**

$E$ (eV)	PBE	$G_0W_0$ <sup>63</sup>	KI <sup>36</sup>	lrLOSC	Exp. <sup>64</sup>
$\langle \varepsilon \rangle_{\text{Li } 1s}$	-40.8	-47.2	-46.6	-47.8	-49.8
$\langle \varepsilon \rangle_{\text{F } 2s}$	-19.5	-24.8	-19.5	-19.7	-23.9
Gap	9.19	14.3	15.28	15.24	15.43

lrLOSC provides a particularly accurate correction for silicon carbide (Figure 3). The qualitative features of the DFA band gap are virtually unchanged, but the electronic gap is adjusted to within 0.04 eV of the correct value. A modest increase in conduction band energies—coupled with a large downward shift in core-level energies, leaving valence energies mostly unchanged relative to the Fermi level—is typical behavior for lrLOSC on the systems tested. In the systems tested, however, the lrLOSC Fermi level is always observed to be

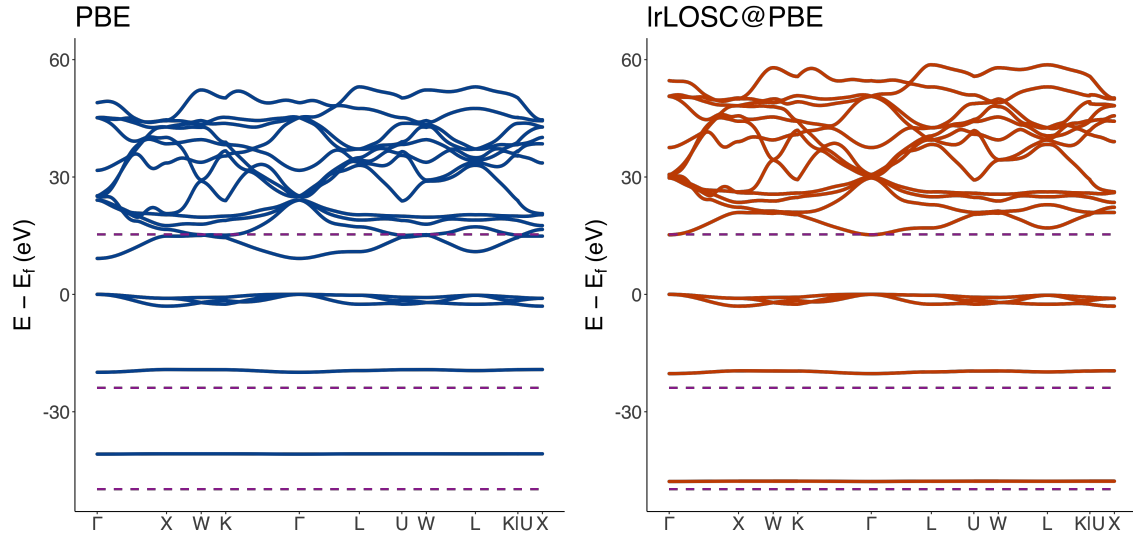


Figure 2: LiF band structure. Purple dashed lines (top to bottom): ZPR-corrected experimental gap, experimental energies for F 2s, Li 1s states.

lower than  $E_F^{\text{PBE}}$ .

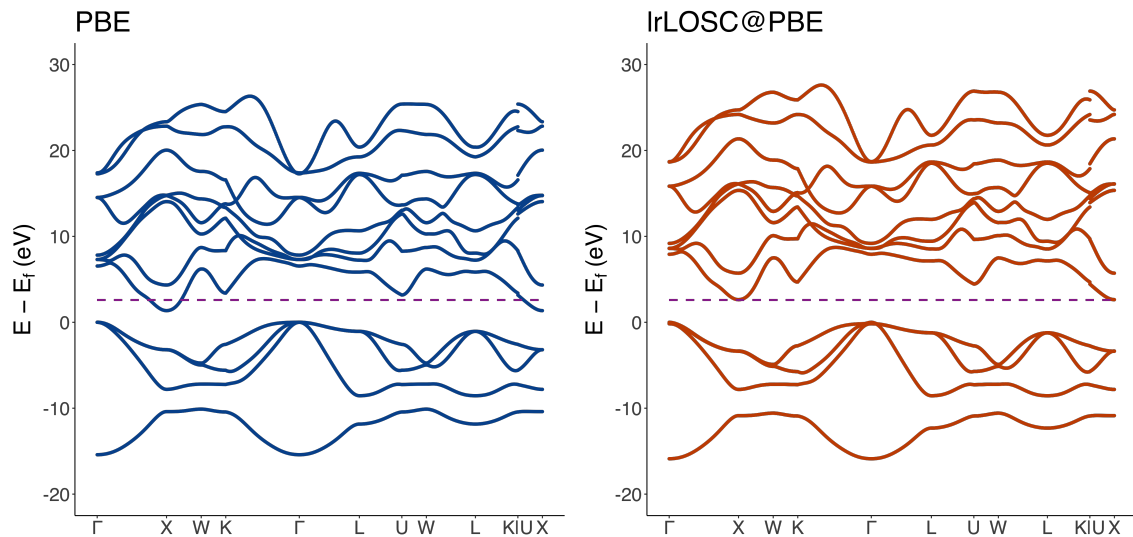


Figure 3: SiC band structure. Purple dashed line: ZPR-corrected experimental gap.

Because it includes both localization and accurate, system-dependent screening, lrLOSC corrects delocalization error effectively in both molecules and materials. It provides accurate, size-consistent orbital and band energy corrections in semiconductors and insulators, matching the performance of many-body perturbation theory without requiring any many-

body observables. Currently, it is limited to gapped systems, as the density response  $\chi$  is not well-defined for metals. Future work will provide curvature applicable to metals that still includes system-dependent screening and implement the self-consistent correction to the density<sup>65</sup> in periodic boundary conditions. With these updates, LOSC will be applicable to interfaces, including molecules on a solid surface. Modeling the energy level alignment of such systems is a major challenge for electronic structure methods,<sup>66–68</sup> and lrLOSC promises a nearly parameter-free solution entirely within the ubiquitous DFT paradigm.

## Acknowledgement

We thank Yichen Fan and Jincheng Yu for helpful discussions of LOSC in molecules, and gratefully acknowledge funding from the National Science Foundation (CHE-2154831) and National Institutes of Health (5R01GM061870-20).

## Supporting Information Available

Details of the monochromatic implementation of linear-response curvature; additional discussion of lrLOSC’s effect on band structures; tests of the monochromatic Coulomb integral against the previous, supercell-periodic implementation; tabulated data underlying Figure 1.

## References

- (1) Hohenberg, P.; Kohn, W. Inhomogeneous Electron Gas. *Phys. Rev.* **1964**, *136*, B864–B871.
- (2) Kohn, W.; Sham, L. J. Self-Consistent Equations Including Exchange and Correlation Effects. *Phys. Rev.* **1965**, *140*, A1133–A1138.
- (3) Levy, M. Universal Variational Functionals of Electron Densities, First-Order Density

- Matrices, and Natural Spin-Orbitals and Solution of the  $v$ -Representability Problem. *Proc. Natl. Acad. Sci. U.S.A.* **1979**, *76*, 6062–6065.
- (4) Levy, M. Electron Densities in Search of Hamiltonians. *Phys. Rev. A* **1982**, *26*, 1200–1208.
- (5) Lieb, E. H. Density Functionals for Coulomb Systems. *Int. J. Quantum Chem.* **1983**, *24*, 243–277.
- (6) Perdew, J. P. Density Functional Theory and the Band Gap Problem. *Int. J. Quantum Chem.* **1985**, *28*, 497–523.
- (7) Perdew, J. P.; Parr, R. G.; Levy, M.; Balduz, J. L. Density-Functional Theory for Fractional Particle Number: Derivative Discontinuities of the Energy. *Phys. Rev. Lett.* **1982**, *49*, 1691–1694.
- (8) Janak, J. F. Proof That  $\frac{\partial E}{\partial N_i} = \epsilon_i$  in Density-Functional Theory. *Phys. Rev. B* **1978**, *18*, 7165–7168.
- (9) Cohen, A. J.; Mori-Sánchez, P.; Yang, W. Fractional Charge Perspective on the Band Gap in Density-Functional Theory. *Phys. Rev. B* **2008**, *77*, 115123.
- (10) Heyd, J.; Peralta, J. E.; Scuseria, G. E.; Martin, R. L. Energy Band Gaps and Lattice Parameters Evaluated with the Heyd-Scuseria-Ernzerhof Screened Hybrid Functional. *J. Chem. Phys.* **2005**, *123*, 174101.
- (11) Xiao, H.; Tahir-Kheli, J.; Goddard, W. A. I. Accurate Band Gaps for Semiconductors from Density Functional Theory. *J. Phys. Chem. Lett.* **2011**, *2*, 212–217.
- (12) Wang, S.; Sakurai, T.; Wen, W.; Qi, Y. Energy Level Alignment at Interfaces in Metal Halide Perovskite Solar Cells. *Adv. Mater. Interfaces* **2018**, *5*, 1800260.

- (13) Li, Y.; Li, Y.-L.; Sa, B.; Ahuja, R. Review of Two-Dimensional Materials for Photocatalytic Water Splitting from a Theoretical Perspective. *Catal. Sci. Technol.* **2017**, *7*, 545–559.
- (14) Ishii, H.; Sugiyama, K.; Ito, E.; Seki, K. Energy Level Alignment and Interfacial Electronic Structures at Organic/Metal and Organic/Organic Interfaces. *Advanced Materials* **1999**, *11*, 605–625.
- (15) Braun, S.; Salaneck, W. R.; Fahlman, M. Energy-Level Alignment at Organic/Metal and Organic/Organic Interfaces. *Advanced Materials* **2009**, *21*, 1450–1472.
- (16) Mori-Sánchez, P.; Cohen, A. J.; Yang, W. Localization and Delocalization Errors in Density Functional Theory and Implications for Band-Gap Prediction. *Phys. Rev. Lett.* **2008**, *100*, 146401.
- (17) Cohen, A. J.; Mori-Sánchez, P.; Yang, W. Insights into Current Limitations of Density Functional Theory. *Science* **2008**, *321*, 792–794.
- (18) Cohen, A. J.; Mori-Sánchez, P.; Yang, W. Challenges for Density Functional Theory. *Chem. Rev.* **2012**, *112*, 289–320.
- (19) Bryenton, K. R.; Adeleke, A. A.; Dale, S. G.; Johnson, E. R. Delocalization Error: The Greatest Outstanding Challenge in Density-Functional Theory. *WIREs Computational Molecular Science* **2022**, *n/a*, e1631.
- (20) Yang, W.; Zhang, Y.; Ayers, P. W. Degenerate Ground States and a Fractional Number of Electrons in Density and Reduced Density Matrix Functional Theory. *Phys. Rev. Lett.* **2000**, *84*, 5172–5175.
- (21) Li, C.; Zheng, X.; Su, N. Q.; Yang, W. Localized Orbital Scaling Correction for Systematic Elimination of Delocalization Error in Density Functional Approximations. *Nat. Sci. Rev.* **2018**, *5*, 203–215.

- (22) Su, N. Q.; Mahler, A.; Yang, W. Preserving Symmetry and Degeneracy in the Localized Orbital Scaling Correction Approach. *J. Phys. Chem. Lett.* **2020**, *11*, 1528–1535.
- (23) Mei, Y.; Yang, N.; Yang, W. Describing Polymer Polarizability with Localized Orbital Scaling Correction in Density Functional Theory. *J. Chem. Phys.* **2021**, *154*, 054302.
- (24) Mei, Y.; Li, C.; Su, N. Q.; Yang, W. Approximating Quasiparticle and Excitation Energies from Ground State Generalized Kohn–Sham Calculations. *J. Phys. Chem. A* **2019**, *123*, 666–673.
- (25) Li, J.; Jin, Y.; Su, N. Q.; Yang, W. Combining Localized Orbital Scaling Correction and Bethe–Salpeter Equation for Accurate Excitation Energies. *J. Chem. Phys.* **2022**, *156*, 154101.
- (26) Zheng, X.; Cohen, A. J.; Mori-Sánchez, P.; Hu, X.; Yang, W. Improving Band Gap Prediction in Density Functional Theory from Molecules to Solids. *Phys. Rev. Lett.* **2011**, *107*, 026403.
- (27) Zhang, D.; Zheng, X.; Li, C.; Yang, W. Orbital Relaxation Effects on Kohn–Sham Frontier Orbital Energies in Density Functional Theory. *J. Chem. Phys.* **2015**, *142*, 154113.
- (28) Yang, W.; Cohen, A. J.; De Proft, F.; Geerlings, P. Analytical Evaluation of Fukui Functions and Real-Space Linear Response Function. *J. Chem. Phys.* **2012**, *136*, 144110.
- (29) Mei, Y.; Chen, Z.; Yang, W. Exact Second-Order Corrections and Accurate Quasiparticle Energy Calculations in Density Functional Theory. *J. Phys. Chem. Lett.* **2021**, *12*, 7236–7244.
- (30) Zhang, D.; Yang, X.; Zheng, X.; Yang, W. Accurate Density Functional Prediction of Molecular Electron Affinity with the Scaling Corrected Kohn–Sham Frontier Orbital Energies. *Molecular Physics* **2018**, *116*, 927–934.

- (31) Yang, X.; Zheng, X.; Yang, W. Density Functional Prediction of Quasiparticle, Excitation, and Resonance Energies of Molecules With a Global Scaling Correction Approach. *Front. Chem.* **2020**, *8*.
- (32) Yu, J.; Mei, Y.; Chen, Z.; Yang, W. Accurate Prediction of Core Level Binding Energies from Ground-State Density Functional Calculations: The Importance of Localization and Screening. <http://arxiv.org/abs/2406.06345>.
- (33) Mahler, A.; Williams, J.; Su, N. Q.; Yang, W. Localized Orbital Scaling Correction for Periodic Systems. *Phys. Rev. B* **2022**, *106*, 035147.
- (34) Nguyen, N. L.; Colonna, N.; Ferretti, A.; Marzari, N. Koopmans-Compliant Spectral Functionals for Extended Systems. *Phys. Rev. X* **2018**, *8*, 021051.
- (35) Colonna, N.; Nguyen, N. L.; Ferretti, A.; Marzari, N. Screening in Orbital-Density-Dependent Functionals. *J. Chem. Theory Comput.* **2018**, *14*, 2549–2557.
- (36) Colonna, N.; De Gennaro, R.; Linscott, E.; Marzari, N. Koopmans Spectral Functionals in Periodic Boundary Conditions. *J. Chem. Theory Comput.* **2022**, *18*, 5435–5448.
- (37) Ma, J.; Wang, L.-W. Using Wannier Functions to Improve Solid Band Gap Predictions in Density Functional Theory. *Sci. Rep.* **2016**, *6*, 24924.
- (38) Weng, M.; Li, S.; Ma, J.; Zheng, J.; Pan, F.; Wang, L.-W. Wannier Koopman Method Calculations of the Band Gaps of Alkali Halides. *Applied Physics Letters* **2017**, *111*, 054101.
- (39) Li, S.; Weng, M.; Jie, J.; Zheng, J.; Pan, F.; Wang, L.-W. Wannier-Koopmans Method Calculations of Organic Molecule Crystal Band Gaps. *EPL* **2018**, *123*, 37002.
- (40) Weng, M.; Li, S.; Zheng, J.; Pan, F.; Wang, L.-W. Wannier Koopmans Method Calculations of 2D Material Band Gaps. *J. Phys. Chem. Lett.* **2018**, *9*, 281–285.

- (41) Weng, M.; Pan, F.; Wang, L.-W. Wannier–Koopmans Method Calculations for Transition Metal Oxide Band Gaps. *npj Comput Mater* **2020**, *6*, 1–8.
- (42) Wing, D.; Ohad, G.; Haber, J. B.; Filip, M. R.; Gant, S. E.; Neaton, J. B.; Kronik, L. Band Gaps of Crystalline Solids from Wannier-localization–Based Optimal Tuning of a Screened Range-Separated Hybrid Functional. *Proc Natl Acad Sci USA* **2021**, *118*, e2104556118.
- (43) Ohad, G.; Wing, D.; Gant, S. E.; Cohen, A. V.; Haber, J. B.; Sagredo, F.; Filip, M. R.; Neaton, J. B.; Kronik, L. Band Gaps of Halide Perovskites from a Wannier-localized Optimally Tuned Screened Range-Separated Hybrid Functional. *Phys. Rev. Mater.* **2022**, *6*, 104606.
- (44) Mahler, A.; Williams, J. Z.; Su, N. Q.; Yang, W. Wannier Functions Dually Localized in Space and Energy. 2022.
- (45) Wannier, G. H. The Structure of Electronic Excitation Levels in Insulating Crystals. *Phys. Rev.* **1937**, *52*, 191–197.
- (46) Marzari, N.; Vanderbilt, D. Maximally Localized Generalized Wannier Functions for Composite Energy Bands. *Phys. Rev. B* **1997**, *56*, 12847–12865.
- (47) Yu, J.; Su, N. Q.; Yang, W. Describing Chemical Reactivity with Frontier Molecular Orbitalets. *JACS Au* **2022**, *2*, 1383–1394.
- (48) Baroni, S.; de Gironcoli, S.; Dal Corso, A.; Giannozzi, P. Phonons and Related Crystal Properties from Density-Functional Perturbation Theory. *Rev. Mod. Phys.* **2001**, *73*, 515–562.
- (49) Timrov, I.; Marzari, N.; Cococcioni, M. Hubbard Parameters from Density-Functional Perturbation Theory. *Phys. Rev. B* **2018**, *98*, 085127.

- (50) Giannozzi, P.; Baroni, S.; Bonini, N.; Calandra, M.; Car, R.; Cavazzoni, C.; Ceresoli, D.; Chiarotti, G. L.; Cococcioni, M.; Dabo, I. et al. QUANTUM ESPRESSO: A Modular and Open-Source Software Project for Quantum Simulations of Materials. *J. Phys.: Condens. Matter* **2009**, *21*, 395502.
- (51) Giannozzi, P.; Andreussi, O.; Brumme, T.; Bunau, O.; Buongiorno Nardelli, M.; Calandra, M.; Car, R.; Cavazzoni, C.; Ceresoli, D.; Cococcioni, M. et al. Advanced Capabilities for Materials Modelling with Quantum ESPRESSO. *J. Phys.: Condens. Matter* **2017**, *29*, 465901.
- (52) Giannozzi, P.; Baseggio, O.; Bonfà, P.; Brunato, D.; Car, R.; Carnimeo, I.; Cavazzoni, C.; de Gironcoli, S.; Delugas, P.; Ferrari Ruffino, F. et al. Quantum ESPRESSO toward the Exascale. *J. Chem. Phys.* **2020**, *152*, 154105.
- (53) Perdew, J. P.; Burke, K.; Ernzerhof, M. Generalized Gradient Approximation Made Simple. *Phys. Rev. Lett.* **1996**, *77*, 3865–3868.
- (54) Hamann, D. R. Optimized Norm-Conserving Vanderbilt Pseudopotentials. *Phys. Rev. B* **2013**, *88*, 085117.
- (55) Gygi, F.; Baldereschi, A. Self-Consistent Hartree-Fock and Screened-Exchange Calculations in Solids: Application to Silicon. *Phys. Rev. B* **1986**, *34*, 4405–4408.
- (56) Mostofi, A. A.; Yates, J. R.; Lee, Y.-S.; Souza, I.; Vanderbilt, D.; Marzari, N. Wannier90: A Tool for Obtaining Maximally-Localised Wannier Functions. *Computer Physics Communications* **2008**, *178*, 685–699.
- (57) Mostofi, A. A.; Yates, J. R.; Pizzi, G.; Lee, Y.-S.; Souza, I.; Vanderbilt, D.; Marzari, N. An Updated Version of Wannier90: A Tool for Obtaining Maximally-Localised Wannier Functions. *Computer Physics Communications* **2014**, *185*, 2309–2310.

- (58) Pizzi, G.; Vitale, V.; Arita, R.; Blügel, S.; Freimuth, F.; Géranton, G.; Gibertini, M.; Gresch, D.; Johnson, C.; Koretsune, T. et al. Wannier90 as a Community Code: New Features and Applications. *J. Phys.: Condens. Matter* **2020**, *32*, 165902.
- (59) Miglio, A.; Brousseau-Couture, V.; Godbout, E.; Antonius, G.; Chan, Y.-H.; Louie, S. G.; Côté, M.; Giantomassi, M.; Gonze, X. Predominance of Non-Adiabatic Effects in Zero-Point Renormalization of the Electronic Band Gap. *npj Comput Mater* **2020**, *6*, 1–8.
- (60) Shang, H.; Zhao, J.; Yang, J. Assessment of the Mass Factor for the Electron–Phonon Coupling in Solids. *J. Phys. Chem. C* **2021**, *125*, 6479–6485.
- (61) Engel, M.; Miranda, H.; Chaput, L.; Togo, A.; Verdi, C.; Marsman, M.; Kresse, G. Zero-Point Renormalization of the Band Gap of Semiconductors and Insulators Using the Projector Augmented Wave Method. *Phys. Rev. B* **2022**, *106*, 094316.
- (62) Lei, J.; Zhu, T. Gaussian-Based Quasiparticle Self-Consistent GW for Periodic Systems. *J. Chem. Phys.* **2022**, *157*, 214114.
- (63) Wang, N.-P.; Rohlfing, M.; Krüger, P.; Pollmann, J. Quasiparticle Band Structure and Optical Spectrum of LiF(001). *Phys. Rev. B* **2003**, *67*, 115111.
- (64) Johansson, L. I.; Hagström, S. B. M. Core Level and Band Structure Energies of the Alkali Halides LiF, LiCl and LiBr Studied by ESCA. *Phys. Scr.* **1976**, *14*, 55.
- (65) Mei, Y.; Chen, Z.; Yang, W. Self-Consistent Calculation of the Localized Orbital Scaling Correction for Correct Electron Densities and Energy-Level Alignments in Density Functional Theory. *J. Phys. Chem. Lett.* **2020**, *11*, 10269–10277.
- (66) Flores, F.; Ortega, J.; Vázquez, H. Modelling Energy Level Alignment at Organic Interfaces and Density Functional Theory. *Phys. Chem. Chem. Phys.* **2009**, *11*, 8658–8675.

- (67) Egger, D. A.; Liu, Z.-F.; Neaton, J. B.; Kronik, L. Reliable Energy Level Alignment at Physisorbed Molecule–Metal Interfaces from Density Functional Theory. *Nano Lett.* **2015**, *15*, 2448–2455.
- (68) Liu, Z.-F. Dielectric Embedding GW for Weakly Coupled Molecule-Metal Interfaces. *J. Chem. Phys.* **2020**, *152*, 054103.